

## **VIII- II -1. Project Research**

### **Project 9**

S. Takahashi

*Research Reactor Institute, Kyoto University*

### Objectives and Allotted Research Subjects

A Fixed-field Alternating-Gradient (FFAG) proton synchrotron (max energy 150 MeV, max mean current 1 nA) has been constructed next to the KUCA to study the technical development for the accelerator driven subcritical reactor (ADSR). The proton beam was led to A-core of the KUCA to conduct the experiment of ADSR on March 4, 2009. On the other hand, the commissioning of a 30 MeV proton cyclotron was completed at the end of March, 2009, for the boron neutron capture therapy (BNCT). And other high energy accelerators are scheduled to conduct as neutron sources in the master plan of KURRI. In these situations, the radiation safety control at accelerator facilities is a key issue in the workplaces and environment.

In these projective studies, five research subjects were carried out in three facilities (the electron linear accelerator, the Co-60 gamma irradiation facility and the proton cyclotron) as substitutes related to the accelerator fields.

The allotted research subjects (ARS) are as follows:

ARS-1 (22P9-1): Development of Passive Neutron Dosimeter with Good Energy Response.

(T. Iimoto, K. Shimada, K. Tani, Y. Fujimichi, K. Yamasaki and T. Takahashi)

ARS-2 (22P9-2): Production and Behavior of Tritium in Accelerator Facilities.

(M. Ohta, S. Kimura, S. Fukutani and K. Okamoto)

ARS-3 (22P9-3): Corrosion of Metals and Colloid Formation in Water under Intense Radiation Field.

(K. Bessho, H. Matsumura, K. Masumoto, Y. Oki, S. Sekimoto, K. Yamasaki, N. Akimoto and N. Osada)

ARS-4 (22P9-4): Nitric Acid Formation and Corrosion of Accelerator Hardware in an Accelerator Irradiation Room.

(Y. Oki, N. Osada and K. Yamasaki)

ARS-5 (22P9-5): Varieties of Radio-Nuclides and Size Distributions of Radioactive Aerosols Produced in Different Types of Accelerators.

(K. Yamasaki, Y. Oki, N. Osada, S. Yokoyama, S. Tokonami, A. Sorimachi, C. Kranrod and S. Takahashi)

### Main Results

ARS-1: The uncertainty of external dose measurements by energy and angular response with dosimeter and worker was discussed using a passive neutron monitor consisted of CR-39 and one millimeter thickness poly-ethylene sheet. If the upper limit of confidence interval was set to 95 % of Cumulative Distribution Function (CDF), in the case of KURRI linac neutron field, the dosimeter value should be set 20 mSv to conform the dose limit of 50 mSv/y.

ARS-2: The concentration of radioactive particles containing of exhaust gases from accelerator for BNCT was continuously measured using a radioactive gas monitor. The concentration of exhaust gas was higher continuously for the limited period of the working of BNCT. The concentration of atmosphere was not affected by the working of BNCT. The tritium compounds from radioactive particles containing of exhaust gases from BNCT appear to be not detected.

ARS-3: In the electron LINAC experiment, the soluble (0-3 nm) and colloidal (3-7, 7-16, 16-200 nm) concentrations of Cu and Fe were measured after irradiation time for 2 h. Dependence of photon intensity on the size profiles showed that high-energy photons promote the transfer of Cu, Fe into water phase. At the <sup>60</sup>Co gamma-ray irradiation to Cu powder/water samples, dominant Cu species in water were colloidal species, which were identified to the copper oxides (Cu<sub>2</sub>O, CuO) by XRD analysis.

ARS-4: Concentration of nitric acid was measured using flow injection analysis in the target room of the Linac facility in KURRI. The nitric acid concentration in the air increased with dose, and about 100 ppm at the irradiation dose of 27 kGy. Eight principal elements, Al, S, Si, Ca, Fe, K, Mo and Zn were detected in the collected dust by the PIXE analysis. The origin of the elements is estimated to be soil from the outside of the facility.

ARS-5: A comparative measurement of the size distributions were conducted in Linac and Cyclotron. Main radio-nuclides were N-13 and Rn-progeny in the Linac target room. On the other hand, those were Mg-27, Na-24 and Rn-progeny in the Cyclotron. The size distributions of Rn-progeny were similar in both accelerators, but those of induced radioactivities such as N-13, Mg-27 and Na-24 from the operation of different types of accelerators were different owing to the operation conditions.

## PR9-1 Development of Passive Neutron Dosimeter with Good Energy Response

T. Iimoto<sup>1</sup>, K. Shimada<sup>2</sup>, K. Tani<sup>2</sup>, Y. Fujimichi<sup>2</sup>,  
K. Yamazaki<sup>3</sup> and T. Takahashi<sup>3</sup>

<sup>1</sup>Division for Environment, Health and Safety, The University of Tokyo

<sup>2</sup>Graduate School of Engineering, The University of Tokyo

<sup>3</sup>Research Reactor Institute, Kyoto University

**INTRODUCTION:** Personal dosimeters which measure photon and neutron are used in many radiation facilities. For example, in high energy accelerators which apply for medical application and nuclear science, radiation workers may be exposed to wide energy range and variety energy spectrum neutron and photon. A passive neutron dosimeter consists usually a combination of PADC (Poly Allyl Digricol Carbonate) and one millimeter thickness polyethylene sheet (PE1). It is hard to measure neutron energy using only PADC with PE1. This dosimeter could not follow changes on personal dose equivalent  $H_p(10)$  [1]. We have been developing passive neutron dosimeter with good energy response in recent years. We are now focusing on practical dose measurement. In dose measurements, measured value has uncertainty. For example, we study dosimeter responses (energy and angular) and their variation during installed with human body. In this research, we discuss uncertainty of external dose measurement by energy and angular response with dosimeter and worker.

**THEORY:** We gave a matrix expression of the relationship between dosimeter response and effective dose equivalent. In case as shown in Figure 1 effective dose equivalent is given as follows [2];

$$D = (b_1 \dots b_n) \begin{pmatrix} a_{11} & \dots & a_{1n} \\ \vdots & \ddots & \vdots \\ a_{n1} & \dots & a_{nn} \end{pmatrix}^{-1} \begin{pmatrix} f_1 \\ \vdots \\ f_n \end{pmatrix} \quad (1)$$

where,  $D$  is effective dose equivalent,  $b_j$  is contribution coefficient of the exposure from  $j$ -th direction to the effective dose equivalent,  $a_{ij}$  is contribution coefficient of the exposure from  $j$ -th direction to the measured value of the  $i$ -th dosimeter, and  $f_i$  is a measured value of the dosimeter facing  $i$ -th direction.

### CALUCULATION and RESULTS:

In this calculation condition, an imaginary worker was exposed from the 4 direction ( $n=4$ ) neutron which has KURRI linac energy spectrum (Fig.2). In addition, we

suppose dosimeter responses are equal to PADC with PE1 which are set around water phantom (30\*30\*15 cm).

Figure.3 shows the calculation results of the Cumulative Distribution Function (CDF) of  $D$  when dosimeter value is 20 mSv. If we set upper limit of confidence interval is 95% of CDF, we should set the limit of dosimeter value is 20 mSv in KURRI linac neutron field to conform the dose limit: 50 mSv per year.

### REFERENCES:

- [1] International Commission on Radiation Protection (1996) "Recommendations of the ICRP Publication 74" Ann. Of the ICRP, 26, No.3/4
- [2] I. ANZAI et al., Japanese Journal of Health Physics (1968)

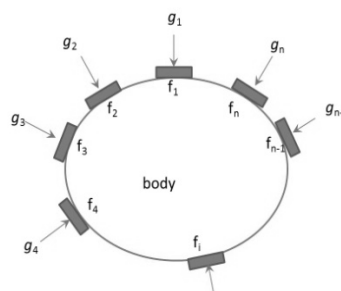


Fig.1. Exposure model.

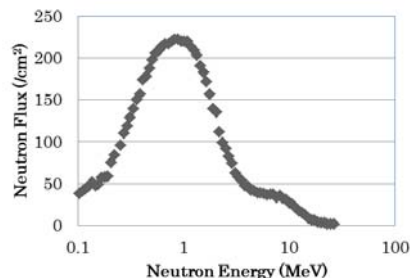


Fig.2. Neutron Spectrum from Ta target by the KURRI LIINAC.

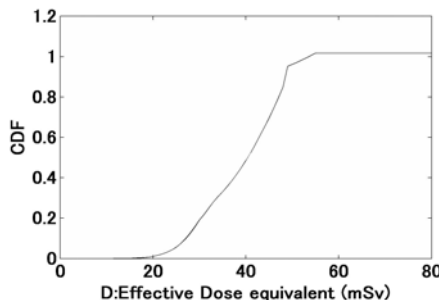


Fig.3. Cumulative Distribution Function of  $D$  by dosimeter value: 20 mSv.

## PR9-2 Production and Behavior of Tritium in Accelerator Laboratory

M. Ohta, S. Kimura<sup>1</sup>, S. Fukutani<sup>2</sup> and K. Okamoto<sup>2</sup>

*Niigata University,*

<sup>1</sup>*Osaka University of Pharmaceutical Sciences,*

<sup>2</sup>*Research Reactor Institute, Kyoto University*

### INTRODUCTION

Radioactive particles are known to generate in the working field of accelerator. Then, the concentration of radioactive particles in the working field of fixed Field Alternating Gradient Accelerator (FFAG) is necessary to be measured before and after working FFAG. However, the concentration of gaseous radioactive particles exhausted from working FFAG in 2010 was too low to be measured as monitoring gas. The present work was measured the concentration of radioactive particles containing of exhaust gases from the accelerator for boron neutron capture therapy (BNCT).

### EXPERIMENTAL

Gaseous radioactive particles were provided from the exhaust gas from the accelerator for BNCT. They were filtered with pre filter and heap filter, and then were used as monitoring gas. The concentration of tritium compounds from radioactive particles containing of exhaust gases from BNCT and atmosphere were measured alternately. The atmosphere outside Innovation Research Laboratory was used as reference gas.

An activity of gaseous radioactive particles was measured by using radioactive gas monitor (Ohkura Electric Co., RD-1,200) and ion chamber (Ohkura Electric Co. I-409602, 1,000cm<sup>3</sup>). The output of ion chamber was digitally recorded by a datalogger (Graphtec Co., midi LOGGER GL200).

### RESULTS

The concentration of radioactive particles containing of exhaust gases from Accelerator for boron neutron capture therapy (BNCT) was continuously measured from February 1 (Tuesday) in 2011 to February 26 (Saturday) in 2011.

Figure 1 shows the concentrations of gaseous radioactive particles contained in the exhaust gas of the neutron generator from February 22 (Tuesday) to February 26 (Saturday) in 2011. The concentration of exhaust gas was higher continuously for the limited

period of the working of BNCT. The concentration of atmosphere was not affected by the working of BNCT.

The tritium compounds from radioactive particles containing of exhaust gases from BNCT appear to be not detected.

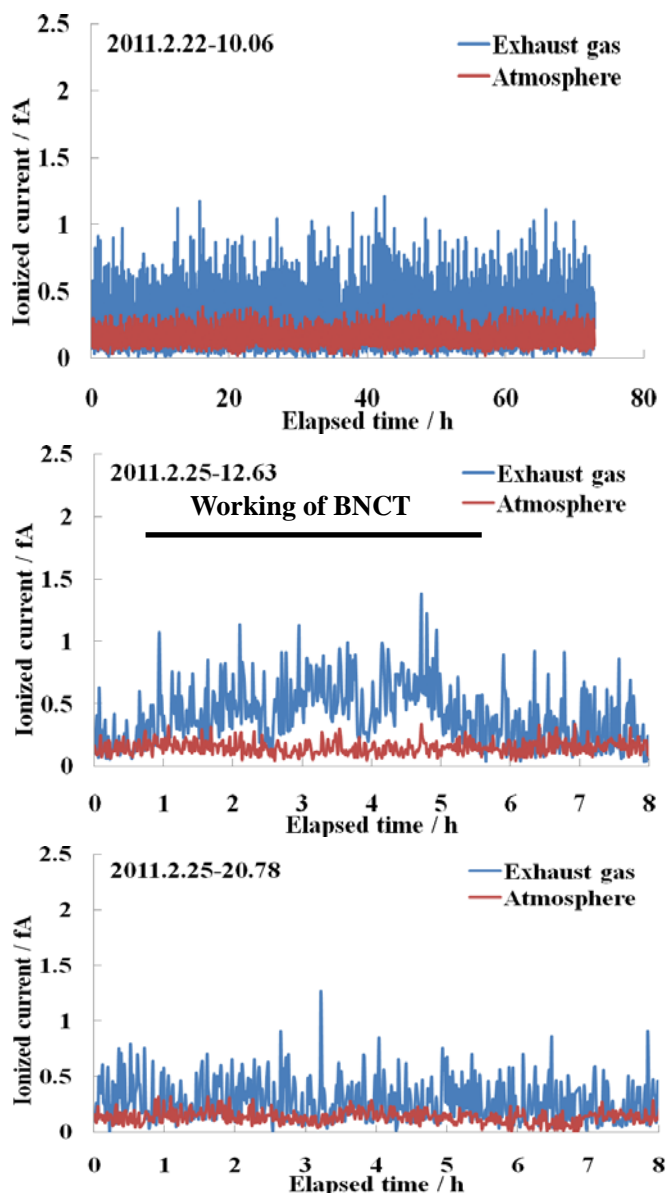


Fig. 1. The concentrations of gaseous radioactive particles contained in the exhaust gas of BNCT and atmosphere outside Innovation Research Laboratory.

K. Bessho, H. Matsumura, K. Masumoto, Y. Oki<sup>1</sup>,  
S. Sekimoto<sup>1</sup>, K. Yamazaki<sup>1</sup>, N. Akimoto<sup>2</sup> and N. Osada<sup>2</sup>

Radiation Science Center, KEK

<sup>1</sup>Research Reactor Institute, Kyoto University

<sup>2</sup>Graduate School of Engineering, Kyoto University

**INTRODUCTION:** At high-intensity accelerator facilities, it is possible that intense radiation fields affect chemical states of metal components around beam-lines and targets. In the cooling-waters for magnets and targets, formation of non-radioactive and radioactive colloids is one of the important subjects in the managements. In this work, metals contacted with water were irradiated by bremsstrahlung and neutrons, or  $\gamma$ -rays, as a model environment inside accelerator facilities. Radiation effects on corrosion and colloid formation were investigated.

### EXPERIMENTS:

#### (1) Irradiations at the electron LINAC

Irradiation was carried out using bremsstrahlung and neutrons generated by 30 MeV electron beam hitting on Ta target ( $\Phi 50 \times 62$  mm) using an electron linear accelerator (LINAC) at the KURRI. A pair of metal containers (I. D. 19x75mm; Pipe materials: Cu, Fe, Al, and so on) filled with pure water was fixed at the downstream position (0 deg: 40 mm from Ta target) and perpendicular position (90 deg: 40 mm from Ta target), as shown in Fig. 1. Electron beam currents were about 23 or 110  $\mu$ A, and the irradiation time was 2 hours.

After the irradiations, water samples in the metal containers were poured out and treated with four kinds filtration (UF) units for particle size separation. Estimated pore sizes of the UF units were 200 nm, 16 nm, 7 nm, and 3nm. Concentrations of metal elements in the filtrates were determined by GF-AAS or ICP-AES analyses.

#### (2) Irradiations at the <sup>60</sup>Co gamma-ray irradiation facility

Pure water (60 ml) and Cu metal powder (1.0 g, 100  $\mu$ m) were sealed into glass vessels, and irradiated by gamma-rays with dose rates of 1.2 kGy/h for 72h or 192h using the <sup>60</sup>Co gamma-ray irradiation facility, KURRI. During irradiation, samples were stirred with a magnetic stirrer. Irradiated samples were treated and analyzed in a similar manner as above.

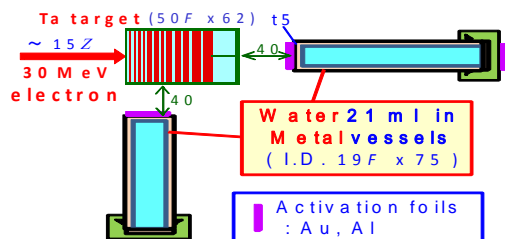


Fig. 1. Experimental setup for the irradiation of the samples at the electron LINAC.

**RESULTS:** In the electron LINAC experiments, intensity of high energy photons, fast neutrons, and thermal neutrons was monitored by activation method using <sup>197</sup>Au( $\gamma, n$ )<sup>196</sup>Au, <sup>27</sup>Al( $n, \alpha$ )<sup>24</sup>Na, and <sup>197</sup>Au( $n, \gamma$ )<sup>198</sup>Au reactions, respectively. Figure 2 shows the soluble (0-3 nm) and colloidal concentrations (3-7, 7-16, 16-200 nm) of Cu and Fe after the LINAC irradiations for 2 h. Dependence of photon intensity on the size profiles clearly shows that high-energy photons promotes the transfer of Cu, Fe into water phase. As for Cu, dominant species induced by radiation was water-soluble species. On the other hand, relatively-large particular species (>200 nm) were dominant after the irradiation on Fe/water targets. The difference between Cu and Fe may reflect hydrolyzed properties of the elements in water.

At the <sup>60</sup>Co gamma-ray irradiation facility, Cu powder/water samples were irradiated by  $\gamma$ -rays for 72h or 192h. After these irradiations, dominant Cu species in water were colloidal species, which were identified to the copper oxides (Cu<sub>2</sub>O, CuO) by XRD analyses. Dependence of the colloidal Cu concentrations on cumulative doses (Fig. 3) imply that irradiation of  $\gamma$ -rays promotes generation of colloidal copper oxides in the time-range of several tens to hundreds hours. Similar results were observed in the experiments which Cu vessels filled with water were irradiated by <sup>60</sup>Co  $\gamma$ -rays.

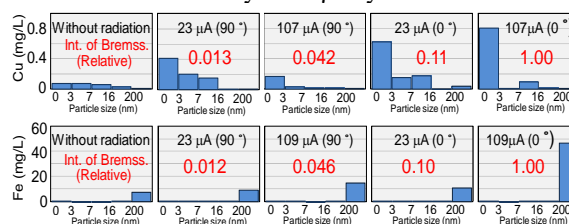


Fig. 2. Soluble (0-3 nm) and colloidal concentrations (3-7, 7-16, 16-200 nm) of Cu and Fe after the LINAC irradiations for 2 h.

Sample : Metal vessels filled with water (I.D. 19 $\Phi$ x75mm)  
Irradiation time : 2 h.

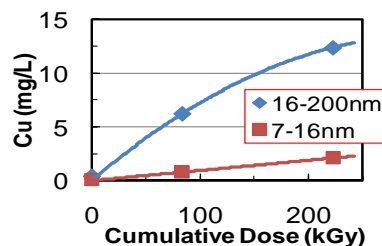


Fig. 3. Dependence of colloidal Cu concentrations on cumulative  $\gamma$ -ray doses from <sup>60</sup>Co source.

Sample : Cu powder (1.0g, 100  $\mu$ m) / Water (60 ml)

Dose rate : 1.2 kGy/h

Irradiation time : 72 h or 192 h.

## PR9-4 Nitric Acid Formation and Corrosion of Accelerator Hardware in an Accelerator Irradiation Room

Y. Oki, N. Osada<sup>1</sup> and K. Yamasaki

Research Reactor Institute, Kyoto University

<sup>1</sup>Graduate School of Engineering, Kyoto University

**INTRODUCTION:** It is well known that oxidizing gaseous species such as ozone, nitrogen oxides and nitric acid are formed through radiolysis processes of air in irradiation rooms of accelerators. Nitric acid is easily adsorbed on the surface of materials. Corrosion of accelerator hardware and peripheral measuring instruments is, therefore, a serious problem for safety of accelerator operation in high-dose radiation accelerators such as electron linear accelerators (linacs) and synchrotron radiation storage rings. Concentration of nitric acid in air is very important information on maintenance of accelerator facilities.

In this work, concentration of nitric acid was determined in a target room of a linac facility. In addition, air dust was sampled in the target room to measure elemental concentration of the dust produced by corrosion of materials in the target room.

**EXPERIMENTS:** Irradiation of air was carried out in the 46-MeV electron linac of Research Reactor Institute, Kyoto University. Glass vessels (100 mL) filled with air (0.1 MPa) were placed around the tantalum target in the target room. The target was bombarded with a 30-MeV electron beam. The beam current was ca. 90  $\mu$ A. During the irradiation, the glass vessels were exposed to bremsstrahlung and neutrons which were produced in the target. L-alanine powder was employed as a dose monitor. After the irradiation, ESR signals of the irradiated alanine were detected to evaluate external doses at the position of the irradiation vessel.

The inside of the irradiated vessel was washed with a small amount of a 0.01 M NaOH solution to extract nitric acid. The extracted nitric acid was determined using a very sensitive flow-injection analysis [1] based on the reduction of nitrate to NO with hydrazine/ascorbic acid and the successive detection of NO by a chemiluminescence NO<sub>x</sub> monitor.

On the other hand, air dust in the target room was sampled for about one week after the beam stoppage. A low-pressure impactor was employed for the sampling to obtain a particle size distribution of elemental concentration of the dust. In the impactor, the dust particles were classified into 14 size ranges, and the classified particles

were collected on polycarbonate filters by impaction. Elemental analysis of the dust on the filter was performed by Particle Induced X-ray Emission (PIXE) at Nishina Memorial Cyclotron Center (NMCC).

**RESULTS AND DISCUSSION:** The radiation doses obtained by the alanine ESR measurement were in the range of 1 to ca. 30 kGy for 4-day operation of the linac. The nitric acid concentration in air increased with an increase in dose. The concentration reached about 100 ppm at the irradiation position near to the target. The dose at the irradiation position was estimated to be 27 kGy. The G-value for the nitric acid formation was roughly estimated to be in the range of 1.5 to 2. It was almost the same as or slightly larger than the reported value of 1.46.[1]

Eight principal elements, Al, S, Si, Ca, Fe, K, Mo, Zn, were detected in the dust by the PIXE analysis. Particle size distributions of Al and S are shown in Fig. 1 along with that of aerosols formed by air radiolysis during machine operation. The origin of the elements are estimated to be soil from the outside of the target room, photochemical reactions of SO<sub>2</sub> and so on. Aluminum showed the highest concentration (8 x 10<sup>-3</sup> ng/cm<sup>3</sup>) among the detected elements. The aluminum dust in the air is considered to be produced by corrosion and friction of aluminum materials.

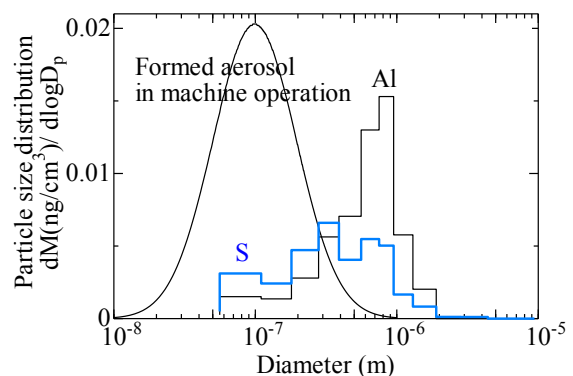


Fig.1. Mass particle size distribution of Al and S in the dust

### REFERENCES:

- [1] Y. Kanda, Y. Oki, S. Yokoyama, K. Sato, H. Noguchi, Su. Tanaka and T. Iida, Radiat. Phys. Chem., **74** (2005) 338-340.

## Varieties of Radio-Nuclides and Size Distributions of Radioactive Aerosol Produced in Different Types of Accelerators

K. Yamasaki, Y. Oki, N. Osada<sup>1</sup>, S. Yokoyama<sup>2</sup>, S. Tokonami<sup>3</sup>, A. Sorimachi<sup>3</sup>, C. Kranrod<sup>3</sup> and S. Takahashi

Research Reactor Institute, Kyoto University

<sup>1</sup>Graduate School of Engineering, Kyoto University

<sup>2</sup>Fujita Health University

<sup>3</sup>National Institute of Radiological Sciences

**INTRODUCTION:** The radiation protection toward the induced airborne particulate radio-nuclides is a key issues for radiation safety of the workers and maintenance of the accelerator facilities. Ultra fine particle generation and particulate radioactivity in high energy and high dose accelerator have been examined using electron linac in this institute. Recently, a proton cyclotron for BNCT has been installed. This report describes mainly the experimental results which were obtained at both accelerators.

**EXPERIMENTS:** Exposure experiments were carried out in the ambient air near target (Ta:Linac, Be:Cyclotron). Both accelerators were operated at the conditions of maximum energy 30 MeV and maximum mean current 90  $\mu$  A to 1mA. Sampling points were about 1 m apart from the target in both cases. At the linac, sample air was introduced to the experimental room with flexible tube made of stainless steel of 2.5 cm dia. and about 6 m in length through radiation shield of 2.5 m thick concrete. At the cyclotron, sample air was introduced to the basement room using flexible tube made of charge proofing rubber of 1.2 cm dia. and about 20 m in length through a labyrinth. Sampling flow rate was about 25  $\ell$  /min. Number and activity-weighted size distributions which were induced high dose and high energy ac-

celerator radiation were measured using SMPS (TSI, Model 3936), CPC (TSI, Model 3025A), laser particle counter (RION, KC-18) and low pressure cascade impactor (Tokyo Dylec, LP-20RS)

The aerosol attached N-13, Mg-27, Na-24 and Rn-progeny were sampled on the 13 stages of the impactor for thirty minutes with flow rate of 22.2  $\ell$  /min. The beta ray from N-13, Mg-27, Na-24 and alpha particles from Rn-progeny were sequentially measured with an automatic sample changer (Aloka, Model JDC-551S) equipped with ZnS(Ag) scintillation counter and GM counter for 1 minute after 15 minutes waiting for the decay of <sup>218</sup>Po. After decay correction, number fractions of radioactive particles were found for each stage of the impactor. Since the size distribution was close to a log-normal distribution, the data of the cumulative fraction vs. the aerodynamic diameter were plotted on a logarithmic probability section paper. The smooth line through those data points was used to find the geometric median diameter (GMD,  $d_g$ ), and geometric standard deviation (GSD,  $\sigma_g$ ).

**RESULTS and DISCUSSIONS:** Table 1 shows typical data of the measured radio-nuclides and their size distributions in the electron Linac and the proton cyclotron in KUR. Both data seems to be somewhat different. Here, N-13 aerosols which exist in the target room of the linac are considered to coexist with largest amount of gaseous N<sub>2</sub> and N-13. On the other hand, Mg-27 and Na-24 are considered to be produced through nuclear reactions of high energy neutron and main constitution of Al near the target material Be in the proton cyclotron.

Table 1. Typical data of the measured radio-nuclides and their size distributions in the electron linac and the proton cyclotron in KUR.

	Electron Linac		Proton Cyclotron		
	N-13	Rn-progeny	Mg-27	Na-24	Rn-progeny
$d_g(\mu\text{m})$	0.21	0.20	0.083	0.084	0.20
$\sigma_g(-)$	1.46	1.46	1.76	1.63	2.15